Experimental aerodynamic investigation of tire geometries

Aleix Lazaro Prat[1,2], Thomas Schütz[1,2], Holger Gau[2]

[1]Institute for Fluid Mechanics and Aerodynamics (SLA), Technical University of Darmstadt,
Peter-Grünberg-Str. 10, 64287 Darmstadt, Germany

[2]BMW AG,
Knorrstr. 147, 80788 Munich, Germany

aleix.lazaro-prat@bmw.de,
thomas.st.schuetz@bmw.de,
holger.gau@bmw.de

Abstract: The objective of this work is to present the advances in the research of the influence of tire geometry features on the drag coefficient of a car. The aim of this holistic analysis is to encompass wind tunnel testing of market-available tires, the development and wind tunnel testing of a modular tire and the evaluation of external flow CFD simulations of cars with accurately deformed tires. From this extensive groundwork, this current publication focuses on the analysis of different market available 245/45 R18 tires on the BMW 4 series and the 5 series touring in the BMW wind tunnel facilities.

1 Introduction

Aerodynamically, tires account for a meaningful share of the total drag coefficient of a car [Schü17, Witt14]. Simulation results from the BMW 4 series showcase that fact, in which it is observed that 10-15% of the total drag share corresponds exclusively to tires [Inte25]. Furthermore, not only they account for a significant share in the C_d, but their geometry changes yield a notable ΔC_d. In the current work, conducted wind tunnel measurements of current market-available 245/45 R18 tires, a maximum $\Delta C_d = 0{,}011$ is observed (BMW 4 series). However, maximum differences up to $\Delta C_d = 0{,}018$ have been experimentally measured in other vehicles (same rim) [Inte25]. This is not an insignificant effect, given that $\Delta C_d = -0{,}001 \approx \Delta range = 1{,}1 - 1{,}5\ km$ on electric cars [HuSo03]. The reason of this influence is the partial exposition of tires to the incoming air, the angle at which the flow impacts the front tires, and the sensitivity of the surrounding (wheelhouse) and downstream geometries (underbody and rear-end). Moreover, and little-known, tires of the same size have a big geometrical spread, in both contour and tread pattern. This fact is studied, together with the wind tunnel results, in the upcoming sections.

Contribution: 2025 FKFS Conference on Vehicle Aerodynamics and Thermal Management
15 – 16 October 2025 | Leinfelden-Echterdingen

The goal of this contribution is to get a clearer understanding of the influence of geometrical features of tires in the total drag coefficient of a car, by experimental means. Few prior studies approach it similarly [HoSe18a, LJWL12, Schn16]. Most of them, however, rely on CFD to evaluate tire aerodynamics [FuUn21, HoSe18b, HoSL13, MSWS21, NaPa25, ReHI19]. This presents several limitations for this use case, besides the ones inherent to the approximations of the simulation: inaccurate tire geometry representation and rotation conditions. They can be accurately tackled, not without a highly resource-intensive structural-aerodynamic simulation [SGBF23]. Therefore, the standard approach in the automotive industry is to simplify the tire geometry and rotation condition.

The following work is structured as thusly: In the method (Section 2) the aerodynamic setup is described, followed by the listing and geometrical analysis of the tested tires. Section 3 presents the results of the wind tunnel tests. These in the discussion section (Section 4). Lastly, an outlook for the research project is briefly debated in Section 5.

2 Method

2.1 Aerodynamic setup

This study has been performed in the BMW aerodynamic wind tunnel. Two different vehicles are considered: the BMW 4 series and 5 series touring, each evaluated in multiple wind tunnel sessions. Results are always presented in deltas relative to a reference and in every wind tunnel session a common (reference) tire set is evaluated to avoid potential variability coming from the wind tunnel calibration. Nonetheless, the repetition of the same geometrical configuration (car and tire set) in different wind tunnel sessions yields a maximum $\Delta C_d = 0{,}001$. If not otherwise stated, the measurements are performed at 140 km/h, with tire pressure of 2,5 bars and standard tire load and vehicle ride height.

Tested tires are exclusively from the size 245/45 R18. All tests are performed with the same rim styling, which is representative of a non-aerodynamically optimized rim. Further exploration of the aerodynamic behavior of tires on other rim stylings is recommended by the authors.

2.2 Tire geometries

The evaluated tires are listed in Table 1 in no particular order. They represent a subset of all 245/45 R18 acquired tires, but only the ones measured in the wind tunnel with a vehicle are included in this study.

To ease readability, each tire has a unique identification code, or ID, assigned in this work (nomenclature *xya*). It includes information on the type (*x*: Summer (SO) =1,

All Season and Winter (A/S) =2) and structure (*y*: Standard (STD) =1 and Runflat (RSC)=2). The third character (*a*) assigns a unique letter for each model.

Table 1: List of the tested 245/45 R18 tires.

ID	Type	Structure	Manufacturer	Model
11A	Summer	Standard	Continental	EcoContact 6 *
11B	Summer	Standard	Pirelli	P Zero *
11C	Summer	Standard	Michelin	Primacy 3 * MO
11D	Summer	Standard	Bridgestone	Turanza T005 *
11E	Summer	Standard	Kumho	Ecsta PS91 * MO
11F	Summer	Standard	Hankook	Ventus S1evo3 *
11G	Summer	Standard	Goodyear	Eagle F1 Asy3 *
12H	Summer	Runflat	Pirelli	Cinturato P7 * (RSC) MOE
12I	Summer	Runflat	Bridgestone	Turanza T005L * (RSC) MOExtended
12J	Summer	Runflat	Hankook	Ventus S1evo3 * (RSC)
22K	All Season	Runflat	Pirelli	Cinturato P7 All Season * (RSC) MOE
12O	Summer	Runflat	Pirelli	P Zero * (RSC)
22P	All Season	Runflat	Pirelli	P Zero A/S (RSC)
11Q	Summer	Standard	Pirelli	P Zero I *
12R	Summer	Runflat	Pirelli	P Zero I * (RSC)
11V	Summer	Standard	Goodyear	Eagle F1 Asy5
21W	Winter	Standard	Pirelli	Winter Sottozero
21X	Winter	Standard	Goodyear	Ultragrip
22Y	All Season	Runflat	Pirelli	P Zero * A/S (RSC)

The addition of type and structure in the identification code is considered relevant, given their influence on the tread measurements and the stiffness of the tire. These two, together with the contour, fully describe its geometry and mechanical properties. The contour is the general curve that is revolved to create the tire. The tread pattern it defined as the embossed cuts used to move the water out of the contact patch. They are divided in longitudinal and side treads. Finally, the structural stiffness refers to the arrangement of steel strings along the perimeter of the tire, designed to withstand the loads. These three are considered by the authors as the entities that explain the shape and behavior of the tire. They are physical independent features that define the final geometry of the deformed tire, in combination with load, camber, toe, pressure and speed.

The geometrical analysis of tires is enabled by the scanning process and subsequent contour and pattern postprocessing developed algorithms (Figure 6 from the Appendix). This workflow outputs the contour and depth image from the tire, which can be processed for further analysis.

2.3 Tire contours

Evaluated tire contours demonstrate a wide design space, depicted in Figure 1. Not only this, but the taxonomy of the contours is as well diverse. Some have an abrupt profile change in the side wall, others present a balloon-like geometry and a few exhibit a trapezoidal format. No shape appears to be predominant over the others.

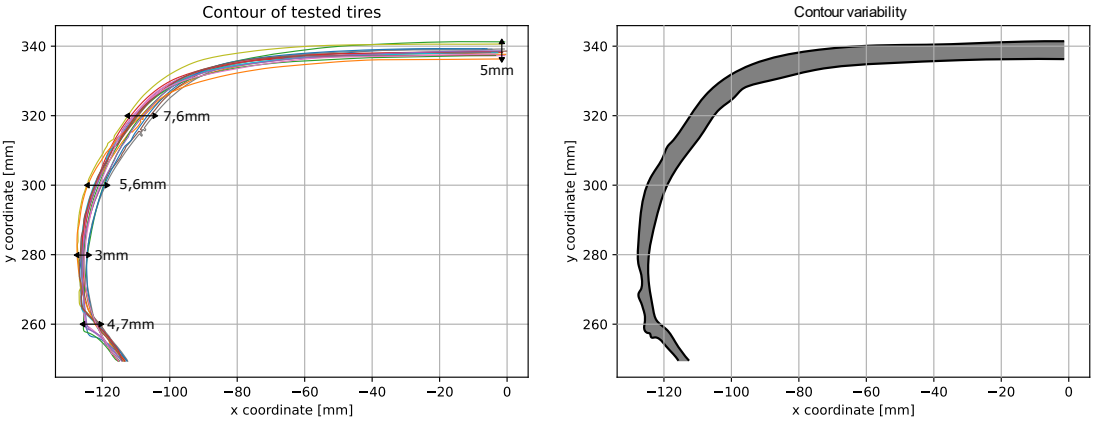

Figure 1: Geometrical variability of the contour of the tested tires, depicted as individual lines on the left-hand side, and their limits on the right-hand side.

Even though most of the contours differ geometrically, a limited number of them are alike. A clustering of the tested tire contours has been performed using a hierarchical agglomerative clustering algorithm. These are: Cluster 1 containing tires 12H and 21W, Cluster 2 with 22P, 12O and 22Y, and Cluster 3 encompassing tires 12J and 11A. They are depicted in Figure 9 from the Appendix. Non clustered geometries do not have comparable contours, emphasizing their diversity. This grouping simplifies the evaluation of drag coefficient delta caused by the tire pattern.

2.4 Tire patterns

Like the contours, the variability in tread patterns designs is substantial, and even more if All Season (or Winter) tires are taken into consideration, like in the presented work.

To enable a characterization of tread geometries that supports the quantitative aerodynamic evaluation of distinct tread components, a feature extraction algorithm is developed. The present approach retrieves exclusively the width and depth of the longitudinal treads. The goal is to identify potential aerodynamic patterns from those, as they dominate the geometry of the pattern. Thus, an automatic vertical line detection algorithm has been implemented. The values for each of the tires, are gathered in Table 2, and the depth maps of the tread patterns are displayed in Figures 7 and 8, all found in the Appendix.

Depending on the pattern shape, the current version of the vertical line detection algorithm might miss a longitudinal tread. This is the case for the foremost left longitudinal tread of the tire 11F, which displays a zigzag silhouette. A more sophisticate approach that embeds the entire pattern shape into a latent space for machine learning-enabled optimization is currently being developed by the researchers.

From the implemented vertical line detecting method, the width and depth distribution of the longitudinal treads are extracted. A simple geometrical analysis shows that, the two parameters do not significantly across tire types. However, the spread in widths is larger for summer standard (SO STD) tires.

Besides the two Winter tires (IDs 21W and 21X), side treads designs do not show apparent geometrical differences. They are slender, shallow similar shapes, positioned at a random (but constrained) distance between each other along the perimeter. This arbitrary distribution avoids the generation of noises, and it adds a layer of complexity in their aerodynamic analysis. In this study they are not considered. In any case, the acoustic requirements of the tires have a higher priority than aerodynamics, and hence any benefit from their aerodynamic optimization in detriment of acoustics would not be justified.

3 Results

This section is structured as follows: First, the base wind tunnel results are discussed. These are tests of the listed tires (Table 1) on the BMW 4 series and 5 series touring under the same inflow velocity (140 km/h) and tire and vehicle conditions (load, tire pressure, rim and ride height). Afterwards, a study on several relevant parameters is presented. Those include tread pattern orientation, ride height, tire pressure, axis position, tire position in vehicle and inflow velocity. In this second part, most of the drag measurements are performed in a reduced number, almost exclusively in the BMW 4 series.

3.1 Base configuration

The results of the aerodynamic evaluation of the tire sets in both the BMW 4 series and 5 series touring are depicted in Figure 2, including the contour clusters highlighted in orange, blue and yellow, respectively. If not otherwise stated, the values are given as deltas relative to the reference tire 12H.

As observed in Figure 2, there is no clear a priori similarity in tire behavior across the two vehicles. Some tires have a similar effect on the ΔC_d (11B, 11G, 11V, 21W, 21X and 22K) and others have not (11C, 11E, 11F, 11Q, 12I). This makes total sense, as the surrounding geometry and flow field are different. However, there might be common geometrical characteristics that on average improve or worsen the C_d.

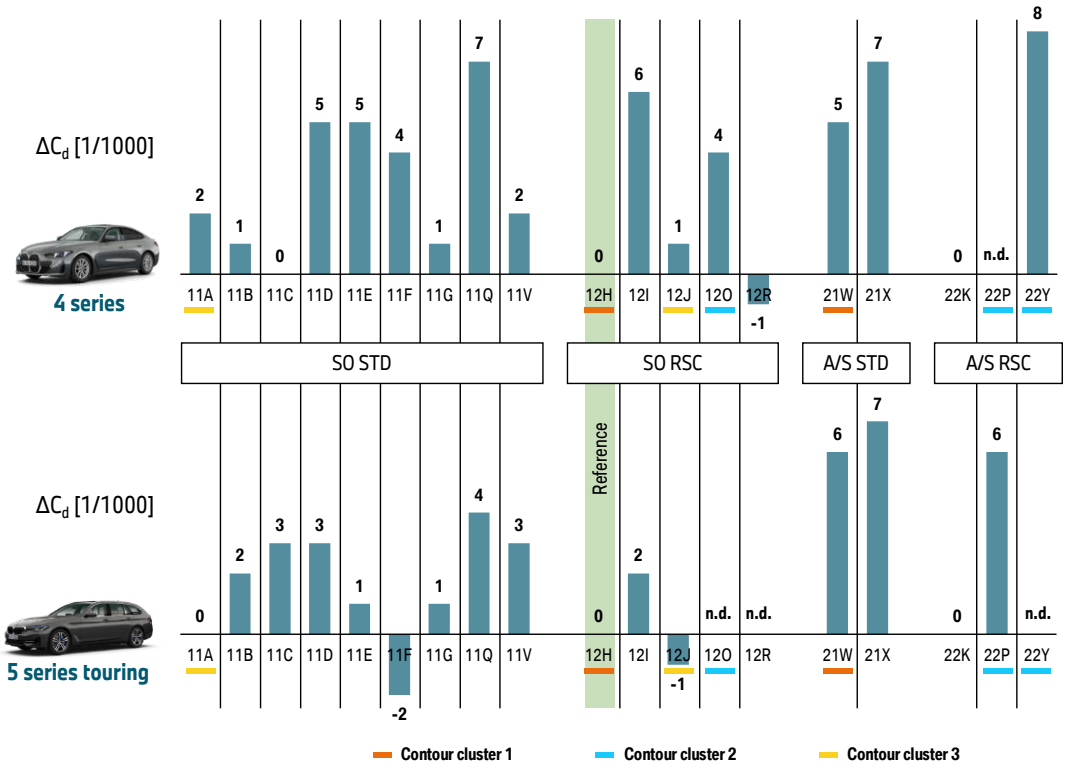

Figure 2: Base wind tunnel results the tested tires with the same rim, tire pressure, load and ride height at 140km/h. Contour clusters are highlighted.

Summer Standard and Runflat tires (SO STD and SO RSC) do not presumably differ in ΔC_d, suggesting that the aerodynamic relevant parameters are embedded in the undeformed shape of the tire. This result does not align with previous tests in different vehicles, in which RSC tires exhibited lower drag due to their stiffer and hence smaller width [Inte25]. Further tests and the analysis of tire scans in the wind tunnel under deformed conditions are required.

Similarly, All Season and Winter tires with both structures (STD and RSC) behave alike in both vehicles. They increase the drag coefficient compared to most of the summer type apart from tire 22K. This model diverges by $\Delta C_d < -0{,}005$ compared to the rest (21W, 21X, 22P and 22Y). Figure 10, located in the Appendix, depicts both contour and tire pattern for such geometries. As observed there, tire 22K has the smallest tire width of the 5 All Season and Winter models, which is expected to be better aerodynamically. Its contour, however, does not considerably differ from tire 21W. In terms of the tread pattern, and with the support of the extracted width and depth, an observation arises: Tire 22K has the maximum longitudinal tread width from them all, and shallow values of depth. These parameters potentially have an influence in the C_d, and thus are further explored.

The results from the contour clusters indicate potential effects caused by the tread pattern. That is the case of Cluster 1. Tire 21W behaves similarly in both vehicles, as tire 12H, but diverge from one another by $\Delta C_d = 0{,}005 - 0{,}006$. Observing 12W, it

contains deeper longitudinal treads than 12H, with a maximum depth of 7,1 mm, fact that seems to be, again, detrimental to the ΔC_d. This effect is observed as well in Cluster 2. Tire 22Y has depths up to 6,6 mm, compared to the 6,1 mm from the 12O. Equally to Cluster 1, deeper grooves seem to not be beneficial for the drag coefficient. Moreover, both geometries from Cluster 2 share the same internal structure (RSC). The opposite however does not seem to strictly hold. The tire with the shallowest longitudinal treads (11A) is not the most aerodynamic one.

If the maximum values of longitudinal depth and width are analyzed, a similar trend is observed: geometries with deeper longitudinal treads yield higher ΔC_d, for both car models. Figure 3 illustrates that trend (colored by contour clusters), alongside the aerodynamic benefit of increasing the width. Note however that these correlations are weak. The experimental analysis of those parameters in an independent manner should be performed to confirm the previous statements.

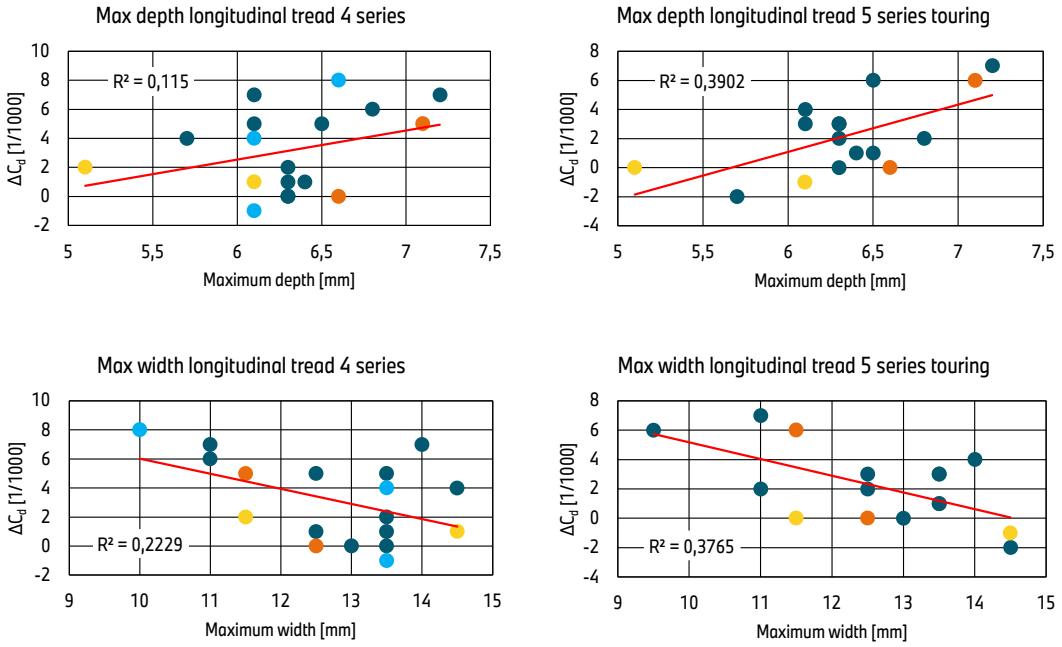

Figure 3: Correlation between maximum width and depth of the longitudinal treads and the ΔC_d, colored by contour cluster.

Analyzing the tires 11Q and 12R, which have similar tread patterns, big differences are observed in the ΔC_d, for the BMW 4 series model. This discrepancy is either originated from the distinct inner structure, or the significant disparity in contour. The second seems the most plausible cause, given the pronounced difference in frontal area. However, the best performing tires (Figure 11, from the Appendix), for both vehicles, share diverse typologies of contours, not necessarily the narrowest ones. They same apply to the contours with tires that produce the highest drag coefficient.

3.2 Pattern orientation

Given the directionality of the tread pattern of tires 21X and 21W, stated by the manufacturer, these have been tested in the opposite configuration in both cars. In doing that, the tire contour and the geometry and position of the longitudinal treads remain constant. The orientation of the side treads is the only modified variable. Results (Figure 6) disguise a clear increase in ΔC_d, clearly exhibiting the relevance of considering these features for aerodynamic optimization. It is unclear if this effect is shared across tire types, as 21X and 21W have a distinguishable deeper side tread layout than the rest. Further tests in other tire types are required to analyze this trend.

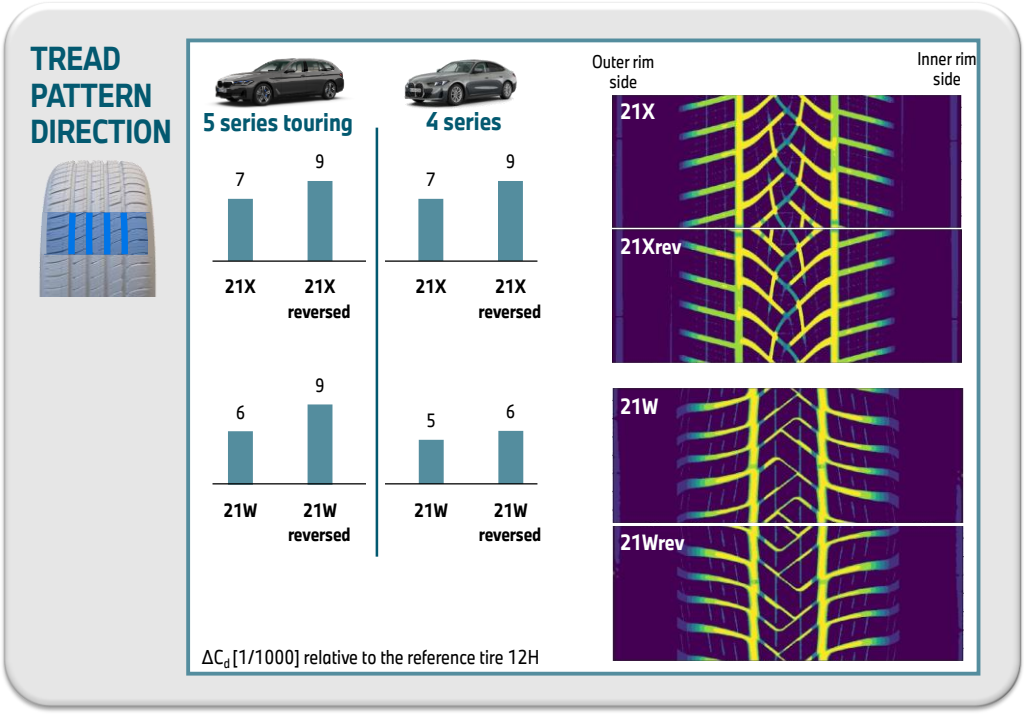

Figure 4: Pattern orientation influence in the ΔC_d.

As tires 21X and 21W in the reverse configuration have the highest recorded drag from the study ($\Delta C_d = 0{,}009$ for both vehicles), they are used to explore the influence of aerodynamically good and bad tires in the front and rear axis (Section 3.6).

3.3 Velocity

Besides the standard testing velocity of 140 km/h, three evaluations have been performed at a reduced speed (100 km/h) in the BMW 4 series. Tires 11A, 21X and 12H have been tested. The objective of this comparison is to assess whether the tires produce a similar outcome at these different speeds. If that is the case, the requirements for the physical modular tire (current under development by the authors) can be lowered.

The results from the experiments show a drag coefficient variation ($\Delta C_{d,140} - \Delta C_{d,100}$) of 0,002, 0 and -0,001, for tires 11A, 21X and 12H, respectively. A more extensive evaluation is required

3.4 Ride height

Tires 12R and 12H have been evaluated under different ride height conditions, to explore the tendency that they follow under the modification of this parameter. Both tires display a very similar behavior, by increasing $\Delta C_d \approx 0{,}005$ every time that the car body is elevated 10 mm.

3.5 Tire pressure

Alongside with the load and the internal structure of the tire, the pressure characterizes the deformation behavior in the contact patch, and in radial due to inertial forces. Hence, the increase in stiffness due to the rise in pressure is expected to cause a reduction in the drag coefficient. Deflated tires exhibit an evidently broader deformation in the contact patch, which increases the frontal area and theoretically generates bigger flow structures that disturb the downstream geometries.

Four different sets have been evaluated in the BMW 4 series (tires 22K, 11B, 12H and 21W), with pressures ranging from 1,8 bars to 3,5 bars. The observed trend is as expected, except for the case of 21W. Nonetheless, all measurements differ by $max\Delta C_d = 0{,}001$, which in the eyes of the authors is not sufficient to generate a statement, and different to previous studies [Inte25]. Like in most of the other variable-studies, the author recommends an extensive analysis of this parameter including scan data from the tire under deformation conditions inside the wind tunnel.

3.6 Axis position

In the following test, two sets of different tires are used: one producing high drag and another a low value of it. Each set is mounted in one of the axes (either the front or the rear), having thus a combined layout. Both BMW 4 series and 5 series touring are included in the experiment. The goal of this evaluation is to determine if there is dominating axis. The selected tires differ 0,007 and 0,009 drag points between them, to better appreciate the effects of the experiment.

A clear dominance of the front axis is observed in the performed measurements, gathered in Figure 7. Front tires receive the impact of the barely disturbed incoming air, which makes their geometry changes more influencing in the aerodynamics of the entire vehicle. Interestingly, the findings are opposite to the wind tunnel results of Landstrom et al. [LJWL12].

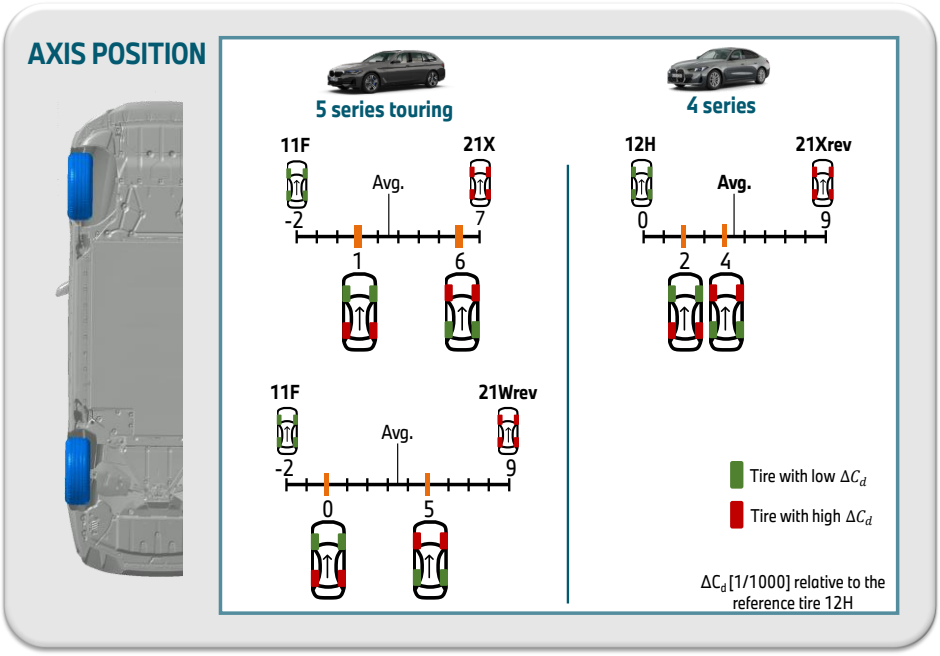

Figure 5: Axis position influence in the ΔC_d.

3.7 Position in the vehicle

Two sets of tires (12H and 12R) are evaluated in the BMW 4 series by placing each individual tire in each of the four positions in the car. This test aims to understand how geometrical tolerances might affect the C_d. Results display a maximum variability of 0,001 in drag coefficient.

4 Conclusions

Tires are multi-parametric multi-requirement complex 3D geometries, that yield a large design space and a substantial spread of drag values. This, complimented by the scarcity of market-available tires from the same size, complicates the aerodynamic evaluation of single geometrical features. However, this work aims to shine some light in the intricate field of tire aerodynamics, from an experimental angle.

The results from the general wind tunnel measurements show a non-equivalence between drag coefficient deltas from the BMW 4 series and the 5 series touring, which is to expect. Most models behave alike, apart from 5 tires (ΔC_d differs by $\geq 0{,}003$).

Summer tires (SO STD and SO RSC) display high variability in both vehicles, with a spread of 0,008 and 0,007 aerodynamic points, for the BMW 4 series and 5 series touring respectively. Winter and All-Season geometries have less spread and a clear higher drag than Summer models, except the ID 22K. This specific geometry exhibits

wide and shallow longitudinal treads, with smaller section area (contour). All these properties could potentially have a beneficial effect in the drag, specially the first two. Further proof is required, as the correlations between these parameters and the ΔC_d are weak. In terms of contour, no design is evidently more beneficial than the rest.

Unexpectedly, no substantial drag difference is observed between STD and RSC across both tire types, nor due to the increase of tire pressure (max. $\Delta C_d = 0{,}001$). This finding should be further studied, as it diverges from previous test [Inte25].

Velocity and ride height behave as expected. The change in air speed and tire rotation modifies slightly the drag coefficient (by $max\Delta C_d = 0{,}002$), and 10mm increments of the ride height increment quite consistently the drag value by approximately 0,005.

Tolerances, which will be always present in the manufacturing, have been briefly evaluated with the testing of tires 12H and 12R in all 4 positions, from the same tire set. Maximum values of 0,001 in drag coefficient have been observed.

Lastly, there is a clear dominance of the front tires on the general trend of the car aerodynamic coefficient. This has been observed in 3 occasions, with $max\Delta C_d = 0{,}005$.

5 Future outlook

Series tires only represent a subset of the design space in which tire manufacturers could potentially manufacture their geometries. Hence, a modular tire is under development by the researchers to fully explore the design space isolating geometrical parameters during the study. The concept intended for the first version of the modular tire is presented in Figure 12. The goal of this prototype is to unveil effects purely coming from the tire tread pattern and not from the contour.

Further research to validate the findings of this work is recommended by the authors. Moreover, a complete description of the tire geometry (including deformation and z-position in the vehicle) could potentially identify features that predominantly govern the drag coefficient. An adequate embedding or parameterization, accounting for of the tire, is therefore vital.

6 Reference list

[FuUn21] Gen Fu, Alexandrina Untaroiu. Investigation of Tire Rotating Modeling Techniques Using Computational Fluid Dynamics. In: *Journal of Fluids Engineering* Bd. 143 (2021), Nr. 11, S. 111206

[HoSe18a] Teddy Hobeika, Simone Sebben. Tyre Pattern Features and Their Effects on Passenger Vehicle Drag. In: *SAE International Journal of Passenger Cars - Mechanical Systems* Bd. 11 (2018), Nr. 5, S. 401–413

[HoSe18b] Teddy Hobeika, Simone Sebben. CFD investigation on wheel rotation modelling. In: *Journal of Wind Engineering and Industrial Aerodynamics* Bd. 174 (2018), S. 241–251

[HoSL13] Teddy Hobeika, Simone Sebben, Christoffer Landstrom. Investigation of the Influence of Tyre Geometry on the Aerodynamics of Passenger Cars. In: *SAE International Journal of Passenger Cars - Mechanical Systems* Bd. 6 (2013), Nr. 1, S. 316–325

[HuSo03] W.-H Hucho, G Sovran. Aerodynamics of Road Vehicles. In: *Annual Review of Fluid Mechanics* Bd. 25 (2003), S. 485–537

[Inte25] *Internal report*: BMW AG, 2025

[LJWL12] Christoffer Landstrom, Linda Josefsson, Tim Walker, Lennart Lofdahl. Aerodynamic Effects of Different Tire Models on a Sedan Type Passenger Car. In: *SAE International Journal of Passenger Cars - Mechanical Systems* Bd. 5 (2012), Nr. 1, S. 136–151

[MSWS21] Mehdi Mortazawy, Richard Shock, Dalon Work, Justin Sacco, James Hoch. Aerodynamic Simulation of a Standalone Round and Deforming Treaded Tire. In: *SAE International Journal of Advances and Current Practices in Mobility* Bd. 3 (2021), Nr. 5, S. 2227–2235

[NaPa25] A Martinez Navarro, G Parenti. Tire Wake Analysis through Unsteady Aerodynamics Simulations. In: *NAFEMS World Congress 2025* (2025)

[ReHI19] Jan Reiß, Lukas Haag, Thomas Indinger. CFD investigation on fully detailed and deformed car tires. In: *International Journal of Automotive Engineering* Bd. 10 (2019), Nr. 4, S. 324–331

[Schn16] Bastian Harald Schnepf. Untersuchung von Einflussfaktoren auf die Umströmung eines Pkw-Rades in Simulation und Experiment (2016)

[Schü17] T. Schütz. Aerodynamische Effizienz von Fahrwerkskomponenten bei zukünftigen Fahrzeugen. In: 2017 — ISBN 978-3-18-102296-2, S. 111–122

[SGBF23] Khaled Sbeih, Arturo Guzman, David Barrera Garcia, Nicolas Fougere, Sam Jeyasingham, Richard Shock, Mehdi Mortazawy, Michael DeMeo. Accurate Automotive Spinning Wheel Predictions Via Deformed Treaded Tire on a Full Vehicle Compared to Full Width Moving Belt Wind Tunnel Results. In: Detroit, Michigan, United States, 2023, S. 2023-01–0843

[Witt14] Felix Wittmeier. *Ein Beitrag zur aerodynamischen Optimierung von Pkw Reifen*. Wiesbaden: Springer Fachmedien Wiesbaden, 2014 — ISBN 978-3-658-08806-4

7 Appendix

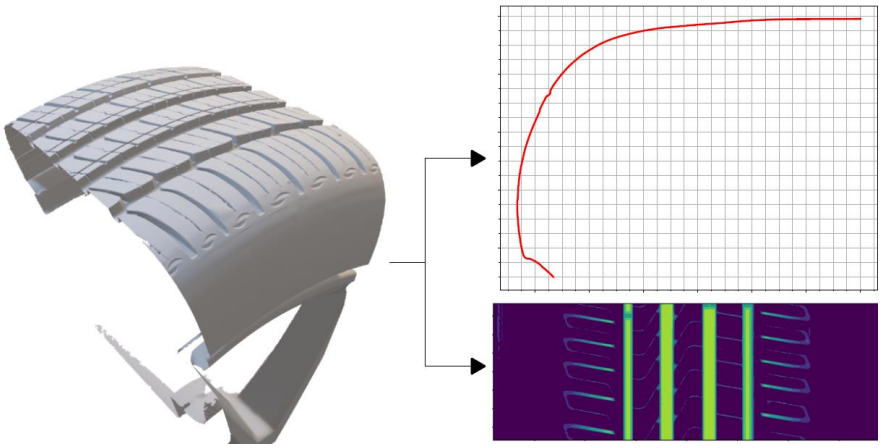

Figure 6: Scanning and geometrical feature identification process.

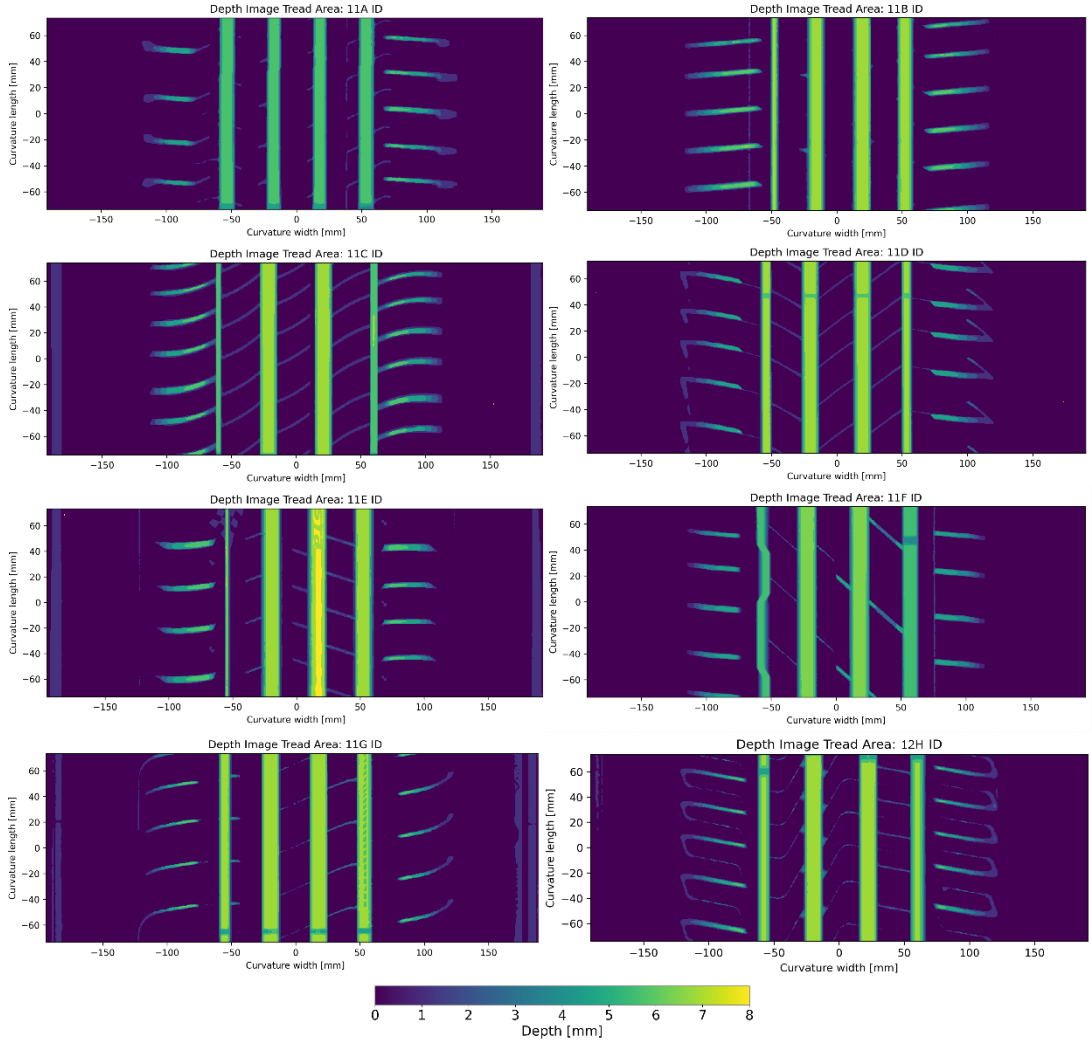

Fig. 7: Tread patterns of tires with IDs from 11A until 12H.

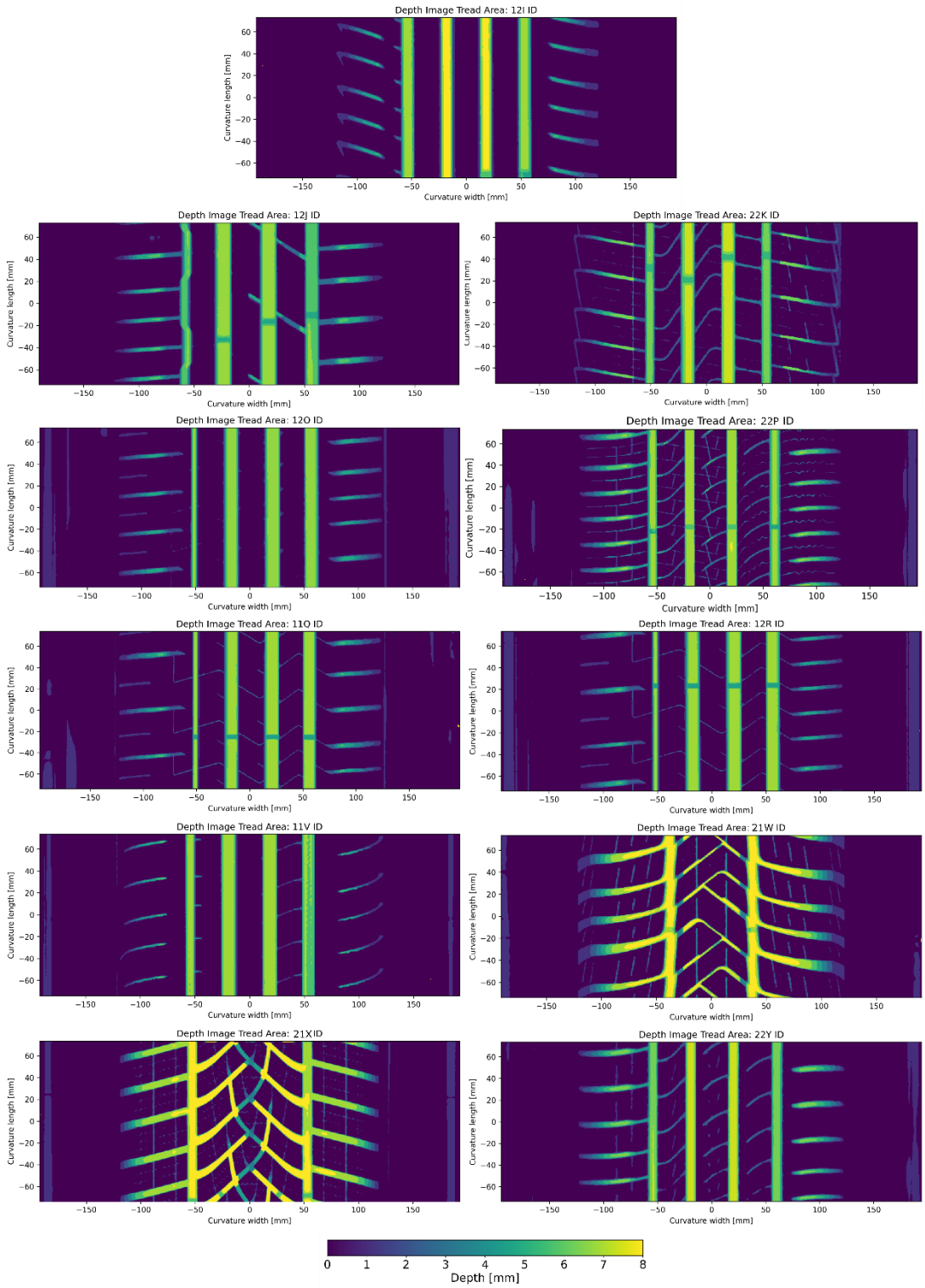

Fig. 8: Tread patterns of tires with IDs from 12I until 22Y.

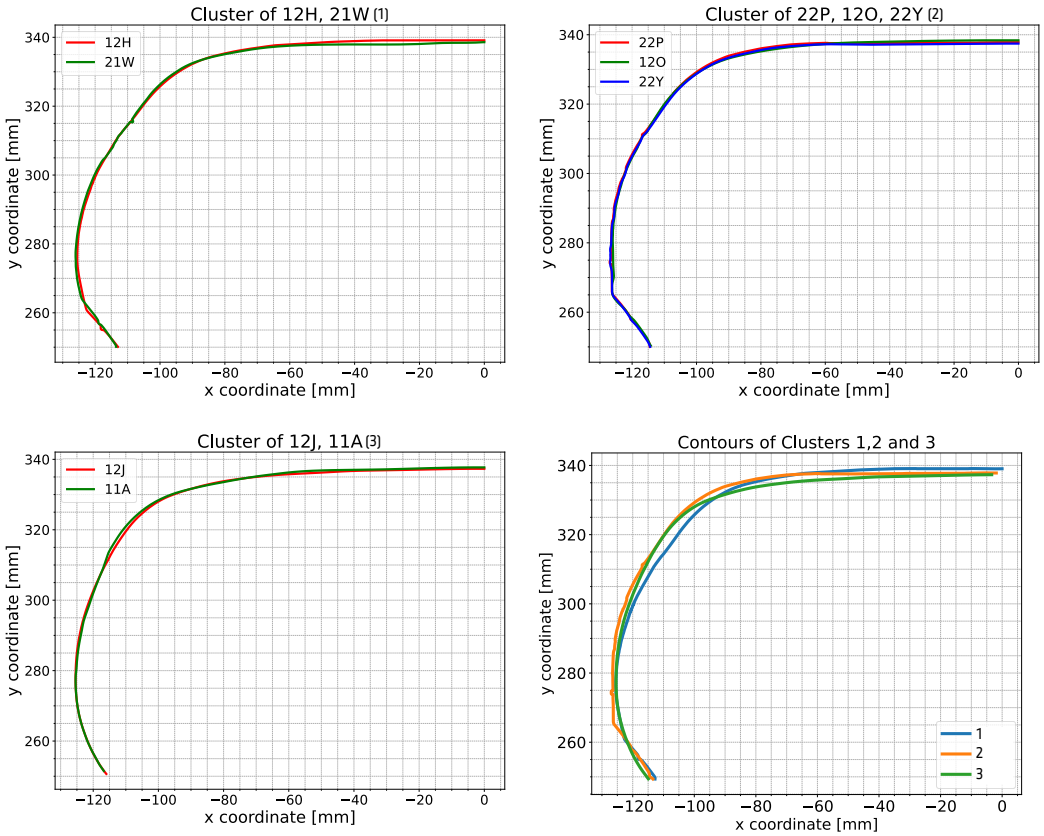

Fig. 9: Contour clusters and comparison between them.

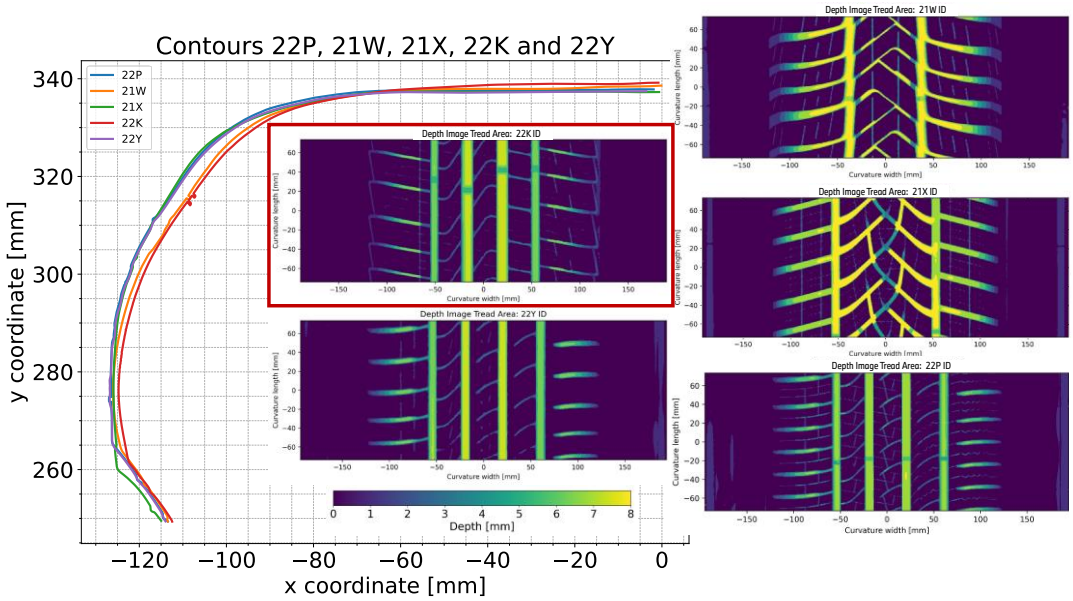

Fig. 10: Comparison of the contours and tread patterns of Winter an All-Season tires.

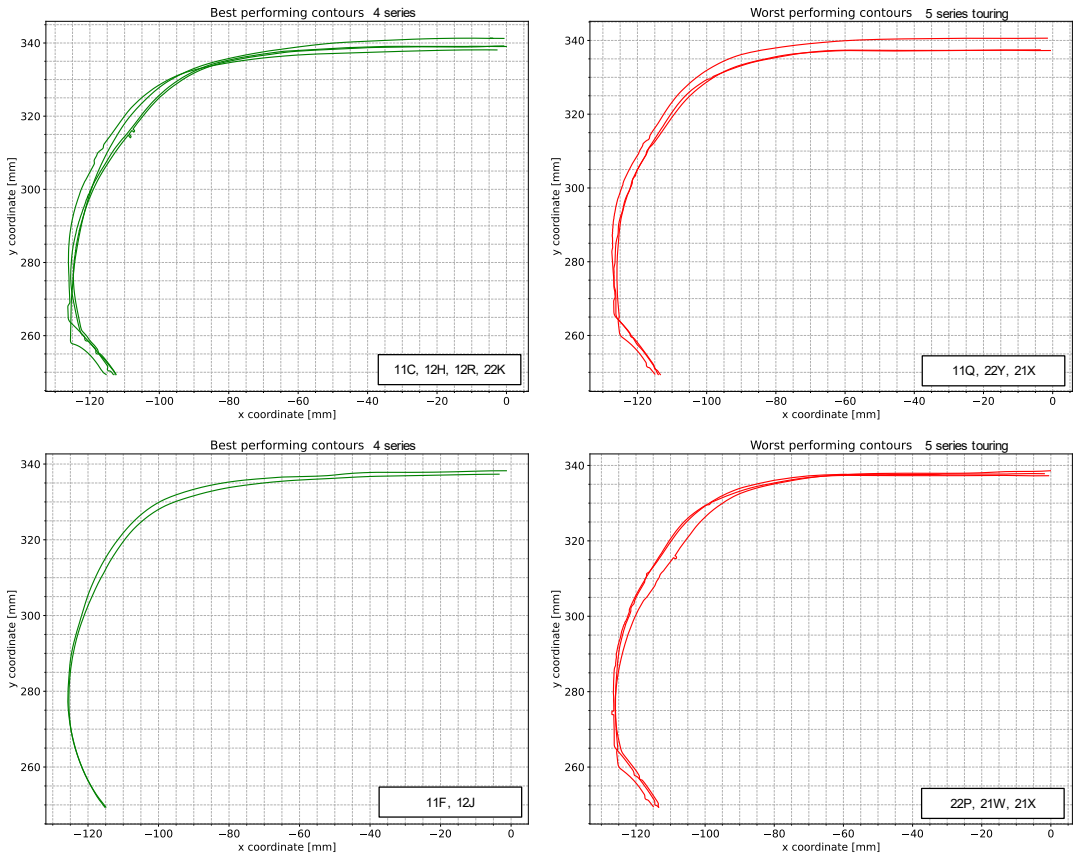

Fig. 11: Best and worst performing tire contours.

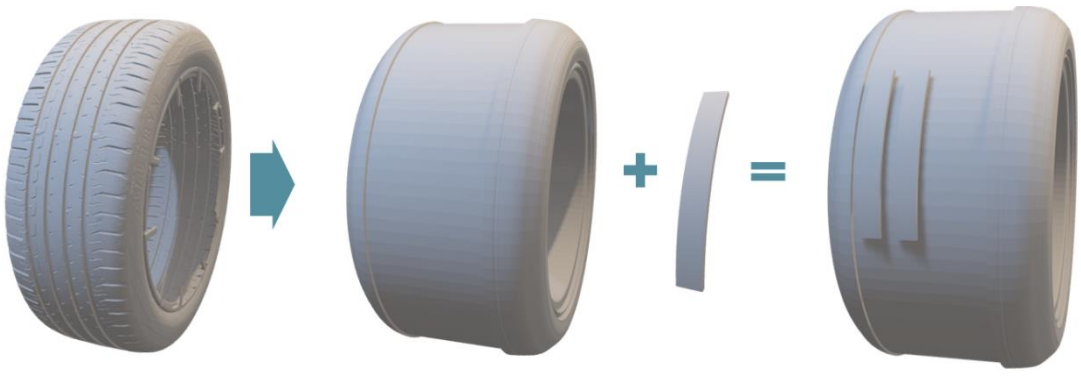

Fig.12: Concept of the modular tire.

Table 2. Base wind tunnel tests, including longitudinal tread width and depth.